RESEARCH ARTICLE

J. Dubois
C. Poupon
F. Lethimonnier
D. Le Bihan

Optimized diffusion gradient orientation schemes for corrupted clinical DTI data sets

J. Dubois · C. Poupon · F. Lethimonnier
D. Le Bihan
Service Hospitalier Frédéric Joliot, CEA,
Orsay, France

J. Dubois · C. Poupon · F. Lethimonnier
D. Le Bihan
IFR49, Paris, France

J. Dubois (✉)
Department of Radiology (CIBM),
Geneva University Hospitals,
Micheli-du-Crest, 24,
1211 Geneva, Switzerland
E-mail: Jessica.Dubois@medecine.unige.ch
Tel.: +41-22-3725216
Fax: +41-22-3824577

Abstract *Object*: A method is proposed for generating schemes of diffusion gradient orientations which allow the diffusion tensor to be reconstructed from partial data sets in clinical DT-MRI, should the acquisition be corrupted or terminated before completion because of patient motion.
Materials and methods: A general energy-minimization electrostatic model was developed in which the interactions between orientations are weighted according to their temporal order during acquisition. In this report, two corruption scenarios were specifically considered for generating relatively uniform schemes of 18 and 60 orientations, with useful subsets of 6 and 15 orientations. The sets and subsets were compared to conventional sets through their energy, condition number and rotational invariance.

Schemes of 18 orientations were tested on a volunteer.
Results: The optimized sets were similar to uniform sets in terms of energy, condition number and rotational invariance, whether the complete set or only a subset was considered. Diffusion maps obtained in vivo were close to those for uniform sets whatever the acquisition time was. This was not the case with conventional schemes, whose subset uniformity was insufficient.
Conclusion: With the proposed approach, sets of orientations responding to several corruption scenarios can be generated, which is potentially useful for imaging uncooperative patients or infants.

Keywords Orientations · Gradients · DTI · Motion · Patient

Introduction

In diffusion tensor (DT) MRI, images must be acquired using diffusion-encoding gradient pulses, applied along at least six non-collinear orientations, to take into account tissue anisotropy [1–4]. As the gradient-encoding scheme may greatly influence the degree to which noise affects the diffusion tensor parameter estimation, several schemes have already been proposed [5–17]. For instance, in order to obtain a uniform distribution of orientations, a model mimicking Coulomb electrostatic interactions [9]

or "ultrarepulsive" interactions [10] has been previously suggested. The evaluation of the condition number of the scheme-associated transformation matrix [11] has been proposed to assess performances regarding sensitivity to noise. A uniform distribution of the orientations in space is necessary to obtain an accurate tensor estimation in each voxel [9,12,13], and the rotationally invariant icosahedra-based sets can provide reproducible results [15–17]. Besides, increasing the orientation count considerably improves the signal-to-noise ratio (SNR) and the diffusion contrast-to-noise ratio [18] by averaging. Considering different orientations then enables a better sampling
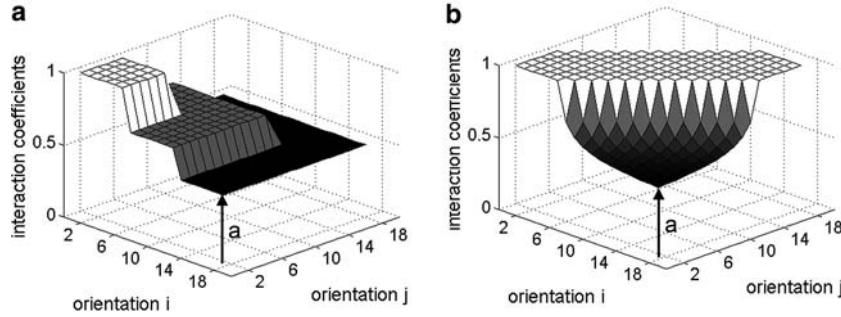
Fig. 1 Interaction coefficients (α_{ij}), as function of orientation positions during acquisition, i and j, for a set of $N = 18$ orientations (subsets of $n = 6$ orientations) with an arbitrary minimum threshold a, for schemes A (**a**) and B (**b**)

of the diffusion space, and, consequently, the information about local tissue organization becomes more accurate [7]. The optimal orientation count to be acquired is still debated and critically depends on the image SNR [10, 13, 14], but the acquisition time linearly increases with this count, and it is not always possible to predict how long a subject (e.g. a non-sedated pediatric patient or an uncooperative patient) will remain still in the MRI scanner. In this case, three acquisition strategies are available for the experimenter.

– He can choose to acquire a *small uniform* set of orientations, during which the patient will surely sleep and which yields an accurate estimation of the diffusion tensor. However, it would not be optimal if the patient continued to sleep after the acquisition end, since more informative data could have been obtained.
– In contrast, he can choose to acquire a *large uniform* set of orientations, but corrupted images should be rejected if motion had happened during acquisition, and the tensor estimation would not be correct with such an incomplete distribution.
– As a *compromise*, he can choose to acquire a *large* set of orientations, which is *not perfectly uniform* but whose *partial subsets* could provide a relatively correct tensor estimation.

In this perspective, our goal was to implement a general method for generating orientation acquisition schemes which yield the "best" spatial distribution of the orientations should motion happen or the acquisition be corrupted or terminated before completion. Thus, our interest was intrinsically different from previous studies [5–17] as we seek a compromise between the available data amount and the diffusion tensor estimation accuracy. In this article, we describe the method of optimization [19] and outline the parameters which can be tuned in order to design schemes for specific motion scenarios. Two examples are given.

Materials and methods

Method description

The method was inspired from a classical model used to generate a spatially uniform distribution of orientations: the physical model of charges distribution on a sphere [9, 10, 12, Appendix 1]. Orientations are assumed to pivot and to repulse each other, through electrostatic forces, and equilibrium is reached when the orientations are uniformly distributed, which corresponds to the minimum of the system global energy. Nevertheless, this model assumes that all of those orientations are available to calculate the diffusion tensor, which in turn implies that the whole data set is intact: if data are corrupted by motion or the acquisition is stopped before completion, the tensor estimation of the undiscarded data will not be very accurate, which implies that the data set may be completely lost.

We propose here to generate schemes of orientations for which partial data sets still contain quite uniformly distributed orientations and can be used for DTI calculation, which is not the case for non-modified "conventional" (uniformly distributed) schemes. In order to generate such schemes, two approaches are available: to sort out the orientation order of a conventional data set [20] or to generate directly an optimized set [19].

With both approaches, an extension to the electrostatic model is necessary. Each orientation is labelled according to its sequential order within the acquisition sequence. The repulsive potential between two orientations i and j, E_{ij}, is proportional to the electrostatic-like potential, E_{ij}^0, (Appendix 1) and to an interaction weight, α_{ij}, which depends on the orientations order: $E_{ij} = \alpha_{ij} E_{ij}^0$. In a uniformly distributed scheme (denoted U), all interactions have equal weights ($\alpha_{ij} = 1$). However, for acquisitions where corruption might occur, the sequence of orientations must consist in a series of small meaningful subsets (a cluster of at least six uniform orientations), while all clusters complement each other with additional orientations. This implies that orientations close in time during the acquisition sequence interact with maximum weight ($\alpha_{ij} = 1$), while orientations distant in time interact with reduced weight ($\alpha_{ij} \leq 1$). The sizes of the whole set and of subsets can be adjusted according to both the programmed total acquisition time and the expected fraction of actually available data. A minimum interaction between the first

Fig. 2 a Normalized energies (*left column*) and condition numbers (*right column*) of sets of 18 orientations and of subsets of m orientations (X_{18}^m, $6 \le m \le 17$, X: A, B or U) for the generated schemes (A_{18}, B_{18}), compared to the non-sorted conventional scheme (U_{18}). Energies and condition numbers were normalized to the energies and condition numbers of the conventional distributions of identical orientation count (U_m). Considering scenario A, the energies and condition numbers of the two first subsets of 6 and 12 orientations (X_{18}^{1-6}, X_{18}^{1-12}, X: A or U) are presented. Considering scenario B, the energies and condition numbers averaged over all the subsets of 6 to 17 orientations (X_{18}^{i-j} with $m = j - i + 1$, X: B or U) are presented. Schemes A_{18}, B_{18} were generated for different minimum thresholds a. **b** Corresponding orientation distributions of the sets of 18 orientations and of some subsets of 6 and 12 orientations for the generated schemes (A_{18}, B_{18}, with $a = 0.5$), compared to the non-sorted conventional scheme U (U_6, U_{12}, U_{18}). **c** Corresponding standard deviations of FA as function of tensor orientation along θ and ϕ
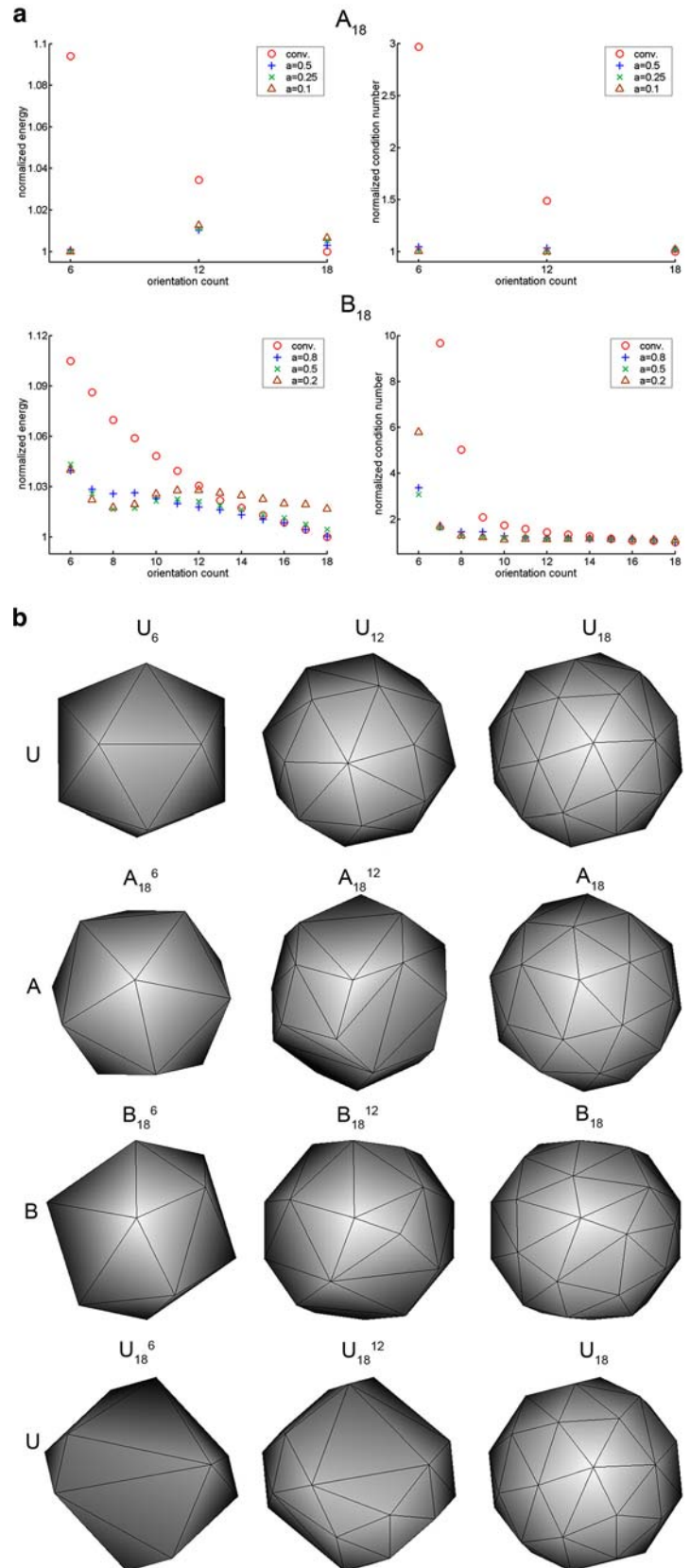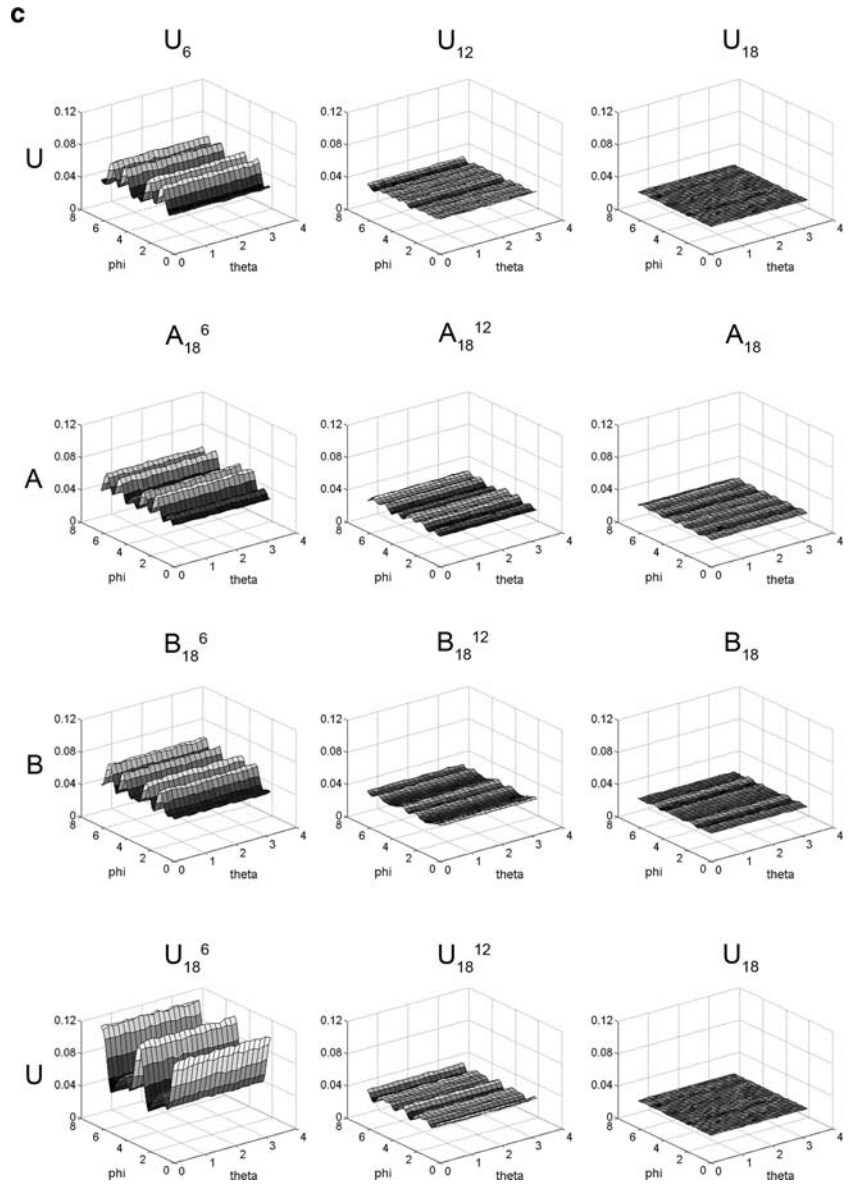
Fig. 2 (Contd.)

and the last orientations provides a coherent global set of orientations, but this threshold may be chosen to give priority to the complete set or to particular subsets. In this way, variable schemes can be devised depending on the expected corruption scenario.

Scheme description

In this article, two different scenarios are presented as examples (Fig. 1, Appendix 2). Sets of N orientations are considered. A threshold ($a \leq 1$) between the first and the last orientations is present in both cases.

In scenario A, the acquisition might be terminated shortly before the expected end (typically a patient is asleep and wakes up) and the scheme is composed of successive subsets of orientations with a small orientation count ($n \geq 6$). A subset is a unit which is completely available or not at all and which must add information compared to previous subsets. In this scheme, interactions within the first subset orientations are maximal, while other interactions decrease with the distance in time between the subsets within the acquisition (Fig. 1a, Appendix 2).

In scenario B, a single acquisition is performed, corruption may occur at any time, at random, but the whole data set is acquired. This scheme assumes that each acquisition segment corresponding to a set of n orientations ($n \geq 6$) is either kept or rejected as a whole. In this scheme, an orientation fully interacts with its $2(n-1)$ closest neighbours in time and the interaction decreases with the distance in time between orientations (Fig. 1b, Appendix 2).

Table 1 Sets of 18 orientations (A_{18}, B_{18}, described in Fig. 2), generated with threshold a = 0.5

Orientations of A_{18}	Orientations of B_{18}
0.609153 0.348325 0.712463	−0.902076 0.426784 0.0641472
−0.787805 −0.52741 0.318123	−0.683024 −0.694914 0.224885
0.0635821 0.989828 0.12727	−0.621315 −0.271961 −0.73485
−0.885332 0.461305 −0.0581836	−0.125341 −0.828559 −0.545691
−0.142819 0.562158 −0.814605	0.181076 0.433856 −0.882599
0.433676 −0.395948 −0.809414	−0.447386 0.325336 0.833068
0.228851 0.850542 −0.473503	0.414791 −0.909039 0.039961
−0.644471 −0.709112 −0.286038	0.95386 0.0833837 −0.288442
−0.446098 0.84138 0.305085	0.803914 −0.447358 0.39191
0.0198736 −0.0799377 −0.996602	0.47033 −0.172819 0.865404
−0.75348 0.308626 −0.580533	−0.695204 −0.650044 −0.306813
−0.871579 −0.0185212 0.489905	0.287343 0.804991 −0.51906
−0.463647 −0.391374 0.794894	−0.0580362 −0.423947 −0.903825
−0.768181 0.47868 0.425163	−0.630117 −0.168543 0.757988
−0.122045 −0.736668 −0.665151	−0.0474071 −0.9914 −0.12198
−0.963215 −0.212488 −0.16452	−0.646892 0.628004 0.432599
0.371772 −0.869556 0.32505	−0.953319 −0.108384 −0.281844
−0.429775 0.112506 −0.895899	0.3372 −0.674455 0.656815

In what follows, we denote by U_N, A_N and B_N the sets of N orientations corresponding to the conventional, non-optimized uniform scheme U and to A and B scenarios. We call X_N^{i-j} any subset of the previous sets (X: U, A or B), with $[i;j]$ the range of orientations in the complete set.

Scheme generation

Given the interaction weights defined for each scenario, the orientation set is optimized from the minimization of its corresponding energy. We used the method which consists in generating directly, as a whole, an optimized set [19]: all orientations were initially randomized and the energy minimization was performed using a conventional descent gradient algorithm [9].

Scheme examples and evaluation

Optimizations were performed with $N/n = 18/6$, for scenarios A and B (for different minimum thresholds a), and $N/n = 60/15$, for scenario A.

The set spatial distributions were characterized by the energy level, calculated with all interaction weights set to 1. The distribution condition number was also assessed. Sets of N orientations (X_N) and subsets of m orientations (X_N^{i-j} with $m = j - i + 1$) were respectively compared to uniform sets of N and m orientations (U_N/U_m) through the normalization of energies and condition numbers. Considering scenario A, respectively two and three subsets were studied (for $N/n = 18/6$, subsets of 6 and 12 orientations: X_{18}^{1-6}, X_{18}^{1-12}; for $N/n = 60/15$, subsets of 15, 30 and 45 orientations: X_{60}^{1-15}, X_{60}^{1-30}, X_{60}^{1-45}). As for scenario B, all subsets of n to $(N-1)$ orientations were considered. Subsets of the non-sorted uniform sets (U_N^{i-j}) were also studied.

Besides, the rotational invariance of the generated sets and subsets was characterized by evaluating the errors in fractional anisotropy (FA) as a function of the tensor orientation [11,13], considering the following parameters: 10^{-3} mm^2 s^{-1} theoretical mean diffusivity, 0.6 theoretical FA, SNR = 30 and $b = 900$ s mm^{-2} (details on the method are provided in [13]). In summary, the tensor was rotated by angle θ around the x-axis from 0 to π (in 20 steps), and angle ϕ around the z-axis from 0 to 2π (in 40 steps). For each rotation, the FA standard deviation was calculated over 5.10^3 samples of noisy signal.

Finally, as an example, a scheme of 18 orientations for scenario A was evaluated on an adult, under a protocol approved by the Institutional Ethical Committee. Four different DTI acquisitions were performed with a DW–SE–EPI technique on a 1.5-T MRI system (Signa LX, GEMS, USA; b value = 0/700 s mm^{-2}, TE/TR = 66.5 ms/12 s, interpolated spatial resolution = $0.9 \times 0.9 \times 3.4$ mm^3). Diffusion gradients were applied according to scheme A_{18} and to schemes U_{18}, U_6 and U_{12} for benchmarking. For $N = 18$ orientations, the acquisition time was 3.8 min. In post-processing, acquisitions corresponding to conventional and proposed schemes were analysed considering either the complete set (the whole acquisition is available) or only subsets of orientations (only a fraction of the acquisition is available); maps of colour-coded directionality (RGB) were calculated.

Results

Sets of 18 orientations (A_{18}, B_{18}) were generated with scenarios A and B, for different minimum thresholds a, and compared to the conventional scheme (U_{18}) (Fig. 2). The normalized energies and condition numbers are presented for the sets and subsets of these schemes (Fig. 2a). Regarding subsets with a small orientation count (m from 6 to 12), the subset corresponding to the conventional scheme strongly differs from the conventional set (U_m) (normalized energies and condition numbers are larger

Fig. 3 a Normalized energies (*left column*) and condition numbers (*right column*) for the sets of 60 orientations and subsets of 15, 30 and 45 orientations for the generated scheme (A_{60}, with $a = 0.5$), compared to the non-sorted conventional scheme (U_{60}). **b** Corresponding orientation distributions. **c** Corresponding standard deviations of FA as function of tensor orientation along θ and ϕ
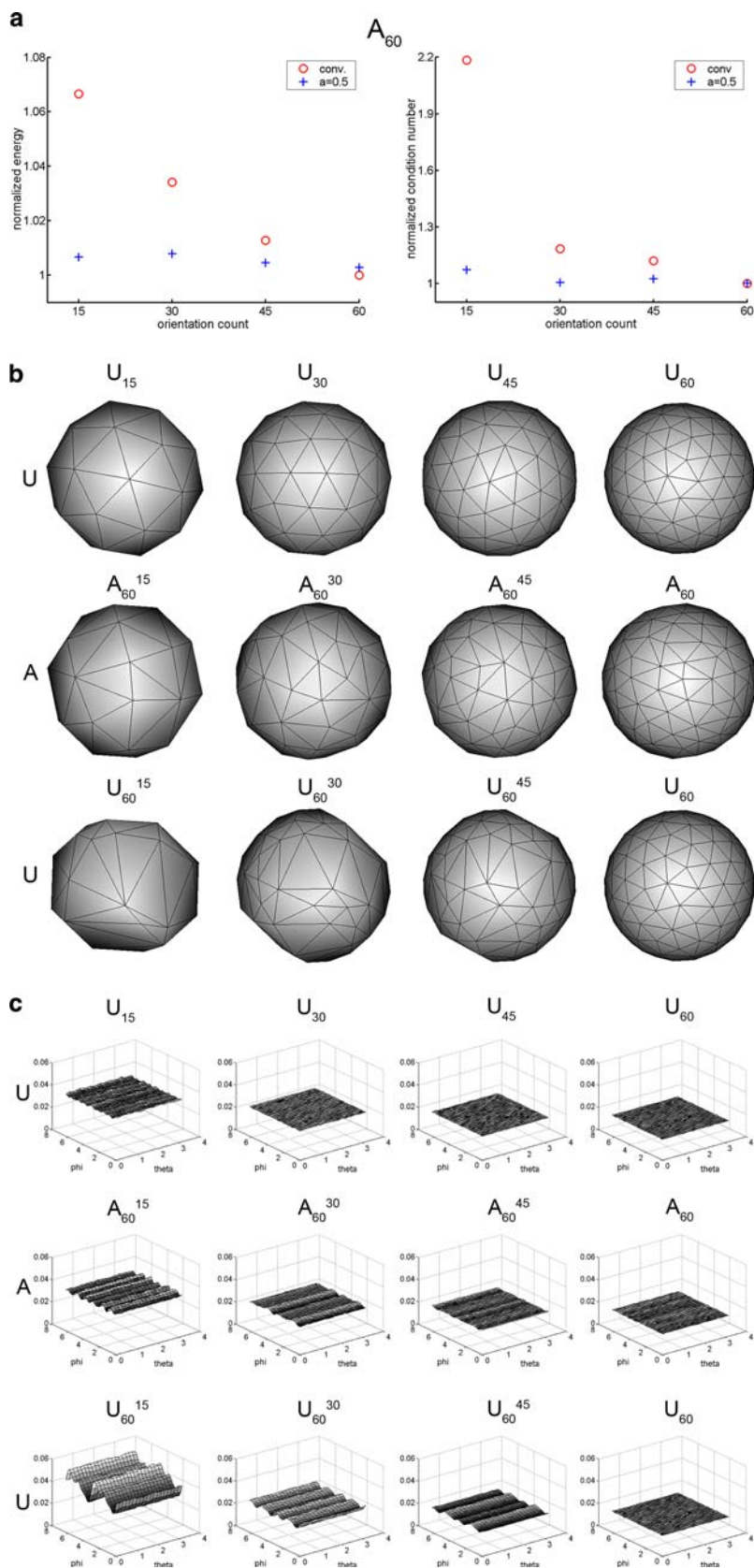
Table 2 Sets of 60 orientations (A_{60}, described in Fig. 3), generated with threshold a = 0.5

Orientation of A_{60}

−0.0620255 0.969279 0.238014
−0.590392 0.691327 0.416539
0.832079 −0.252625 −0.493787
0.407539 0.753135 −0.51643
0.772251 0.321716 −0.547839
−0.399355 0.0182789 0.916614
0.542116 −0.22155 0.810571
−0.144761 −0.260138 −0.954658
0.96726 −0.193975 0.163652
−0.0996349 0.965323 −0.241297
−0.721408 −0.457627 −0.519757
−0.0431366 0.498168 −0.866007
−0.62369 −0.780281 −0.0466048
0.698702 −0.677253 0.23053
−0.0794753 −0.666166 −0.741557
−0.415908 0.908961 0.0284565
−0.516029 0.517755 −0.682381
−0.312844 0.355545 0.880748
−0.200541 0.792286 −0.576252
−0.908794 0.365036 0.202096
0.0661257 0.187804 −0.979978
−0.274626 −0.954691 0.11465
0.356633 0.477761 −0.802843
0.828767 0.0218569 −0.559167
0.837099 0.517716 0.176735
−0.279575 0.819499 0.500259
0.65698 0.203892 0.725814
0.956585 0.257488 −0.13655
−0.397375 −0.721049 −0.567611
−0.895454 0.0165788 −0.444845
0.289479 −0.6167 −0.73204
−0.243609 −0.951229 −0.189256
−0.442904 −0.138527 −0.885803
−0.22214 0.207392 −0.952703
−0.705832 0.699695 0.110576
0.426922 −0.850603 0.306939
0.613782 0.723288 0.316425
−0.990266 −0.0921729 −0.104297
0.0927022 0.723476 −0.684097
−0.606186 0.403811 0.685183
−0.538433 −0.790268 0.292515
−0.541466 −0.216562 0.812352
0.354366 0.499081 0.790786
0.812979 −0.370855 0.448922
−0.788945 −0.501919 0.354461
−0.624942 0.625522 −0.467086
−0.0389319 0.998982 0.0227983
0.478208 −0.820052 −0.314375
0.821955 0.555657 −0.125045
0.153939 0.905929 −0.394456
−0.642144 0.0829743 0.76208
0.189207 0.852312 0.487611
0.585638 0.513825 −0.626907
−0.0934106 0.0619547 0.993698

Table 2 (Contd.)

Orientation of A_{60}

0.0452882 −0.484571 −0.873579
0.881691 −0.471656 0.0126873
0.72787 −0.114571 0.676076
0.250884 −0.583763 0.77219
0.878214 0.296705 0.375109
−0.977722 0.0155313 0.209331

than 1). In contrast, the subsets for scenarios A and B are acceptable (normalized energies and condition numbers are close to 1). For subsets with a larger orientation count (12 to 17), the trend is the same while the difference in quality is less pronounced. This means that if an acquisition is corrupted before completion (e.g. in case of motion), the implemented orientation schemes allow the data sets to still be meaningful and usable, which would not be the case with a conventional acquisition scheme. When we compare the whole sets, the generated schemes are equivalent to the conventional one in terms of global space sampling, which means that no information is lost if the acquisition is not interrupted. As scenario B is more flexible than scenario A with regard to the acquisition hypothesis (corruption can happen at any time, not just at the acquisition end), sets B_{18} and the B subsets of 6 and 12 orientations are respectively less optimal than sets A_{18} and the A subsets.

As outlined for each scenario, the choice for threshold a results from a trade-off between the distribution uniformity for the whole set and subsets, which cannot be optimal for both. The threshold should be iteratively optimized by the user according to the expected acquisition scenario. In the next part, we focus on the distributions generated for an intermediate threshold ($a = 0.5$).

Distributions of sets A_{18} and B_{18} and of some subsets are presented in Fig. 2b and Table 1. As expected, the FA rotational invariance is improved with set uniformity (Fig. 2c). For both the generated sets and subsets, it is close to the optimal situation (complete uniform set). In addition, the FA standard deviation decreases as the orientation count increases.

In Fig. 3 and Table 2, results obtained with scenario A for a set of 60 orientations (A_{60}) with a minimum subset of 15 orientations are described.

Figure 4 represents diffusion maps obtained on a volunteer, highlighting the corpus callosum body, in different situations (interruption of the acquisition before completion or not) for schemes A_{18} and U_{18} compared to U_6 and U_{12}. Maps obtained with scheme A_{18} are very similar to those obtained with conventional distributions, both with the full set or a subset, but results are significantly different with the conventional scheme U_{18}.
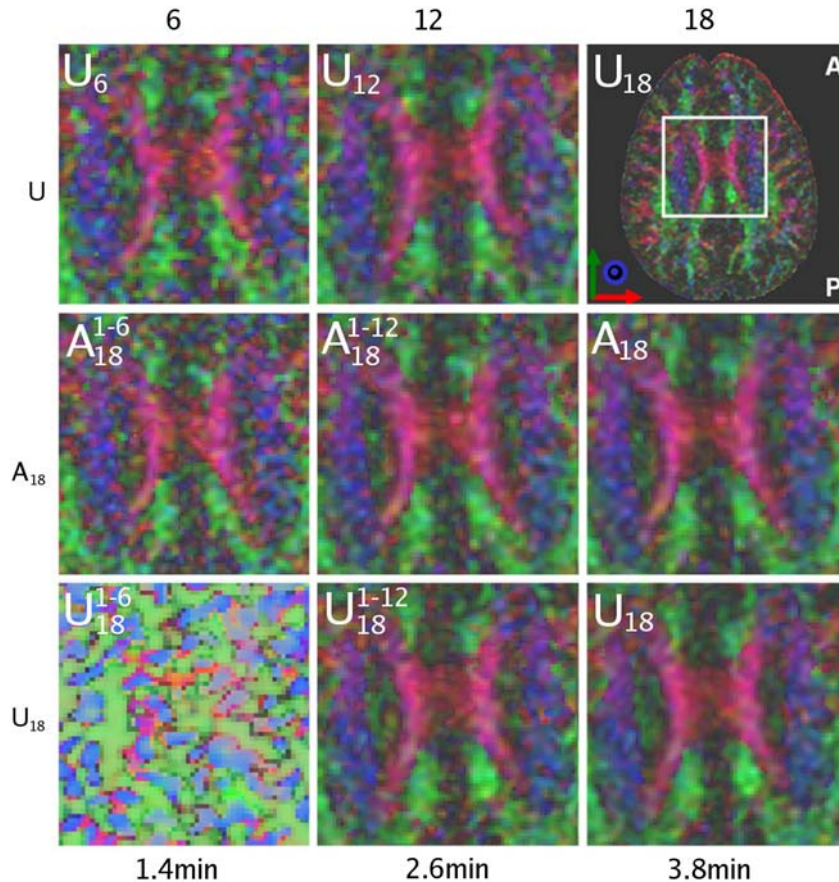
Fig. 4 RGB maps obtained on a volunteer (zoomed at the level of the body of the corpus callosum) using 6, 12 and 18 orientations of conventional schemes U and scheme A_{18}(U_6, U_{12}, X_{18}^{1-6}, X_{18}^{1-12}, X_{18}, X: A, U), with corresponding acquisition time

Discussion and conclusion

Since the time a patient can remain still in an MRI scanner is not always predictable, especially with non-sedated infants or uncooperative patients, our goal was to implement a method for generating orientation schemes, for DTI acquisitions, which permit one not to lose the whole data set in case of motion or if the acquisition is stopped before programmed completion. A compromise must be found between an optimized spatial distribution of orientations (and so the tensor estimation accuracy, [5–17]) and a somewhat short acquisition time. Our minimization method was inspired by a model based on Coulomb electrostatic interactions [9], but different interaction coefficients between orientations were introduced according to their sequence order within the acquisition sequence in order to generate subsets of orientations which maintain a uniform distribution in space.

Whereas several scenarios can be designed using this method, two examples were specifically detailed in this article. Examples obtained for schemes of 18 and 60

orientations were described. We focused on acquisition schemes applicable, for instance, to unsedated babies, with high robustness to motion, short acquisition time and small orientation count. The generated sets were compared with conventional ones by characterizing their energy and their condition number, as these indexes were shown to be respectively markers of the spatial uniformity of the distribution [9] and of the noise performance for the DTI scheme [11]. The FA rotational invariance was also briefly evaluated for the generated sets, but it was beyond the scope of this article to quantitatively assess the robustness of the generated schemes concerning tensor estimation [13,16]. Diffusion maps were presented for one of the set examples: their quality was only slightly modified when only subsets were used.

As previously outlined, two approaches were available to deal with acquisition with potential early termination. One approach [20] was to sort out the orientation order in a complete set of uniform orientations, so that the first acquired orientations are the more uniformly distributed over the space. Nevertheless, "recycling" a uniform set is not optimal for generating uniform subsets, and

two optimization cycles must be successively performed, which is time consuming. Moreover, these sorted sets are inappropriate in the case of *random* corrupted acquisitions (case B). In contrast, with the proposed approach [19], orientations were not fixed and the constraint was directly applied in the first optimization. By design, this approach was more optimal for generating uniform subsets and it was therefore preferred, even though the global set of orientations was not necessarily uniform as in the first approach.

Interestingly, with our method, orientation schemes can be dedicated to specific scenarios or subject population. However, the scenario must be defined *before* the acquisition so as to program the necessary gradient orientation temporal sequence within the acquisition, and subsets with unartefacted images are selected in post-processing. Also the orientation optimization becomes more complicated with large orientation counts, and it is difficult to optimize both small and large subsets. Therefore, a first step with the proposed approach is to precisely define the scenario which must be dealt with in order to generate an appropriate orientation distribution.

In conclusion, we proposed a general approach to generating clinically useful sets of orientations and we outlined the parameters which can be tuned in order to design schemes for specific corruption scenarios. The executable code for generating such orientation sets (NmrUniformOrientationSet) is freely available on the laboratory website (http://brainvisa.info).

Appendices

Appendix 1: Generation of uniform distributions

To generate a spatially uniform distribution of orientations, the analogy with the physical model of charges distribution on a sphere has been suggested [9]. The global energy, E, of a system of N orientations is minimized:

$$E = \sum_{\substack{i,j=1 \\ i<j}}^{N} E_{ij},$$

where E_{ij} is the interaction potential between orientations i and j.

As acquiring in DTI an orientation ($\vec{g}_i$) or its symmetrical counterpart ($-\vec{g}_i$) is equivalent, both are considered for the calculation of the electrostatic-like potential (E_{ij}^0):

$$E_{ij}^0 \propto \frac{1}{\|\vec{g}_i - \vec{g}_j\|} + \frac{1}{\|\vec{g}_i + \vec{g}_j\|}.$$

Appendix 2: Interaction weights

– Case A

In this scenario (Fig. 1a), a subset of orientations ($S+1$) includes the previous subset (S). S is defined as the smallest subset that orientations i and j both belong to. The more distant in time the orientations are, the more reduced is the interaction. If i and j belong to the first subset ($S = 1$), their interaction is maximal: $\alpha_{ij} = 1$. If i and j belong to the last subset ($S = P$, with P the number of subsets), their interaction is minimum: $\alpha_{ij} = a < 1$. Otherwise, the interaction coefficient is defined as $\alpha_{ij} = a^{(S-1)/(P-1)}$.

Note that many other schemes, not detailed here, can be devised on this thematic. If a subset of orientations is not assumed to include the previous one, the interaction coefficient can be defined as $\alpha_{ij} = a^{|I-J|/(P-1)}$, where orientations i and j belong respectively to subsets I and J. In addition, for generating small independent uniform subsets (without constraints of time) and a uniform set, the coefficient can be defined as $\alpha_{ij} = \delta_{IJ} \cdot (1-a) + a$, where δ_{IJ} is the Kronecker symbol. In the method proposed by Cook et al. [20], a is null because the global set is the conventional (uniform) one.

– Case B

In this scenario (Fig. 1b), an orientation fully interacts with its $2(n-1)$ closest neighbours in time: if $|i - j| < n$ then: $\alpha_{ij} = 1$. For the most distant orientations (the first and the last), the interaction is minimum: $\alpha_{1N} = a < 1$. Otherwise, the interaction monotonically decreases as the distance in time ($|i - j|$) increases: if $|i - j| \geq n$

$$\alpha_{ij} = 1 - (1-a) \cdot \frac{N-n+1}{N-n} \left(1 - \frac{1}{|i-j|-n+2}\right).$$

References

1. Le Bihan D, Mangin JF, Poupon C, Clark CA, Pappata S, Molko N, Chabriat H (2001) Diffusion tensor imaging: concepts and applications. J Magn Reson Imag 13:534–546
2. Basser PJ (1995) Inferring microstructural features and the physiological state of tissues from diffusion-weighted images. NMR Biomed 8:333–344
3. Basser PJ, Mattiello J, Le Bihan D (1994) Estimation of the effective self-diffusion tensor from the NMR spin echo. J Magn Reson B 103:247–254
4. Basser PJ, Mattiello J, Le Bihan D (1994) Diffusion tensor tensor spectroscopy and imaging. Biophys J 66:259–267
5. Conturo TE, McKinstry RC, Akbudak E, Robinson BH (1996) Encoding of anisotropic diffusion with tetrahedral gradients: a general mathematical diffusion formalism and experimental results. Magn Reson Med 35:399–412
6. Basser PJ, Pierpaoli C (1998) A simplified method to measure the diffusion tensor from seven MR images. Magn Reson Med 39:928–934
7. Papadakis NG, Xing D, Huang CL, Hall LD, Carpenter TA (1999) A comparative study of acquisition schemes for diffusion tensor imaging using MRI. J Magn Reson 137:67–82
8. Papadakis NG, Xing D, Houston GC, Smith JM, Smith MI, James MF, Parsons AA, Huang CL, Hall LD, Carpenter TA (1999) A study of rotationally invariant and symmetric indices of diffusion anisotropy. Magn Reson Imag 17:881–892
9. Jones DK, Horsfield MA, Simmons A (1999) Optimal strategies for measuring diffusion in anisotropic systems by magnetic resonance imaging. Magn Reson Med 42:515–525
10. Papadakis NG, Murrills CD, Hall LD, Huang CL, Carpenter TA (2000) Minimal gradient encoding for robust estimation of diffusion anisotropy. Magn Reson Imag 18:671–679
11. Skare S, Hedehus M, Moseley ME, Li TQ (2000) Condition number as a measure of noise performance of diffusion tensor data acquisition schemes with MRI. J Magn Reson 147:340–352
12. Hasan KM, Parker DL, Alexander AL (2001) Comparison of gradient encoding schemes for diffusion-tensor MRI. J Magn Reson Imag 13:769–780
13. Batchelor PG, Atkinson D, Hill DL, Calamante F, Connelly A (2003) Anisotropic noise propagation in diffusion tensor MRI sampling schemes. Magn Reson Med 49:1143–1151
14. Jones DK (2004) The effect of gradient sampling schemes on measures derived from diffusion tensor MRI: a Monte Carlo study. Magn Reson Med 51:807–815
15. Akkerman EM (2003) Efficient measurement and calculation of MR diffusion anisotropy images using the Platonic variance method. Magn Reson Med 49:599–604
16. Hasan KM, Narayana PA (2003) Computation of the fractional anisotropy and mean diffusivity maps without tensor decoding and diagonalization: theoretical analysis and validation. Magn Reson Med 50:589–598
17. Madi S, Hasan KM, Narayana PA (2005) Diffusion tensor imaging of in vivo and excised rat spinal cord at 7 T with an icosahedral encoding scheme. Magn Reson Med 53:118–125
18. Xing D, Papadakis NG, Huang CL, Lee VM, Carpenter TA, Hall LD (1997) Optimised diffusion-weighting for measurement of apparent diffusion coefficient (ADC) in human brain. Magn Reson Imag 15:771–784
19. Dubois J, Poupon C, Cointepas Y, Lethimonnier F, Le Bihan D (2004) Diffusion gradient orientation schemes for DTI acquisitions with unquiet subjects. In: Proceedings of the 12th annual meeting of ISMRM, #443
20. Cook PA, Boulby PA, Symms MR, Alexander DC (2005) Optimal acquisition order of diffusion-weighted measurements on a sphere. In: Proceedings of the 13th annual meeting of ISMRM, #1303